Effect of the Hepatocyte-Specific Deletion of SND1 in Mice on the Liver Insulin Resistance and Acute Liver Failure

Chunyan Zhao
Tianjin Medical University
Xiaoteng Cui
Tianjin Medical University
Baoxin Qian
Tianjin Medical University
Nan Zhang
Tianjin Medical University
Lingbiao Xin
Tianjin Medical University
Chuanbo Ha
Tianjin Medical University
Jie Yang
Tianjin Medical University
Xinting Wang
Tianjin Medical University
Xingjie Gao (gaoxingjie@tmu.edu.cn)
Tianjin Medical University https://orcid.org/0000-0002-3287-7697

Research article

Keywords: high-fat diet, insulin resistance, liver conditional knockout, SND1

Posted Date: July 27th, 2020

DOI: https://doi.org/10.21203/rs.3.rs-48660/v1

Abstract

Background: The multifunctional protein SND1 was reported to be involved in a variety of biological processes, such as cell cycle, proliferation or lipogenesis. We previously proposed that global-expressed SND1 *in vivo* is likely to be a key regulator for ameliorating HFD-induced hepatic steatosis and systemic insulin resistance. Herein, we are very interested in investigating further whether the hepatocyte-specific deletion of *SND1* affects the insulin resistance or acute liver failure (ALF) of mice.

Methods: By using Cre-loxP technique, we constructed conditional knockout (LKO) mice of *SND1* driven by albumin in hepatocytes and analyze the changes of glucose homeostasis, cholesterol level, hepatic steatosis and hepatic failure under the treatment of high-fat diet (HFD) or upon the simulation of Lipopolysaccharide/galactosamine (LPS/GalN).

Results: No difference for the body weight, liver weight, and cholesterol level was detected. Furthermore, we did not observe the alteration of glucose homeostasis in *SND1* hepatic knockout mice on either chow diet or high-fat diet. Besides, hepatocyte-specific deletion of *SND1* failed to influence the hepatic failure of mice induced by LPS/GalN.

Conclusions: These findings suggest that hepatic SND1, independently, is insufficient for changing glucose homeostasis, hepatic lipid accumulation and inflammation. The synergistic action of multiple organs may contribute to the role of *SND1* in insulin sensitivity or inflammatory response.

Background

In human, SND1 (staphylococcal nuclease and tudor domain containing 1), also known as Tudor-SN (Tudor staphylococcal nuclease), includes four staphylococcal nucleases-like (SN1 ~ SN4) domains of N-terminus and one Tudor-SN5 (TSN) domain of C-terminus [1, 2]. After on a series of assays based the cellular, animal or clinical samples, SND1 was reported to be involved in a variety of biological processes, including lipogenesis, splicing of mRNA precursors, cell cycle, gene transcription, DNA damage repair, proliferation, tumorigenesis, etc. [3–12]. With regards to the SND1 expression-associated animal models, only global *SND1* transgenic mice and hepatocyte-specific *SND1* transgenic mice (Alb/SND1 mice) [13] were reported [14]. Herein, we first generated mice with the hepatocyte-specific deletion of *SND1* in the liver, namely an *SND1* liver conditional knockout mice model, and investigated the role of *SND1 in vivo* in the issues of liver Insulin resistance and acute liver failure (ALF).

As an essential organ *in vivo*, the liver tissue is critical to the occurrence of insulin resistance and acute liver failure [15, 16]. Emerging studies reported the functional links between SND1 and liver tissue in different species. For instance, human SND1 can promote the proliferation of hepatocellular carcinoma cell lines [12, 17], and contributes to the occurrence of hepatocellular carcinoma [13, 18]. SND1 protein was reported to promote the secretion of lipoprotein phospholipids in primary hepatocytes of rats [19, 20]. Very recently, we also observed the reduced accumulation of triglyceride and the improved fatty liver and insulin resistance in the liver tissue of global *SND1* transgenic mice under the treatment of a high-fat diet

[14]. In this study, we are thus very interested in investigating further whether hepatocyte-specific deletion of *SND1* in mice affects the presence of insulin resistance induced by a high-fat diet.

Acute liver failure (ALF) is a clinical syndrome that involves sudden and massive liver cell death and liver dysfunction, resulting in coagulopathy, encephalopathy and circulatory dysfunction, thereby leading to multiple organ failure [21, 22]. It was reported that the over expression of SND1 was associated with a chronic inflammatory state of leading to hepatocellular carcinoma cell [13].Nevertheless, the relationship between*SND1* expression and acute inflammation in the liver remains elusive. Thus, we also investigated whether the hepatocyte-specific deletion of *SND1* influences the acute liver failure process using a Lipopolysaccharide (LPS)-induced mice model of ALF in galactosamine (GalN)-sensitized mice.

Methods

SND1 liver conditional knockout mice

The *SND1 Flox/ Flox* mice were first constructed in our laboratory and then crossed with albumin-Cre$^+$ mice with the *wild type* (*wt*) allele of *SND1* (*wt/ wt*-albumin-Cre$^+$ mice, The Jackson Laboratory, USA) to produce the *SND1 Flox/ wt*-albumin-Cre$^+$ heterozygous mice. After the second round of mating, we obtained the *SND1 Flox/ Flox*-albumin-Cre$^+$ homozygous mice, which were used as the *SND1* liver conditional knockout (LKO) mice. *SND1 Flox/ Flox* littermates were used as wild type (WT) controls.

To verify the successful construction of *SND1* LKO mice, we extracted the DNA from mouse primary hepatocytes and performed the genotyping PCR assay to detect the presence of *SND1 Flox* sites and the Cre gene. Primers were synthesized by the GENEWIZ Company (China). The primer sequences used were: *SND1 Flox* 5′-CAGCACTAAAAGCTTGTCCC-3′ (forward 1, F1), 5′-ACGAGAGTATGGGATGATCT-3′ (forward 2, F2), 5′-GCTAAAGAGTCCCTAGAAAG-3′ (reverse, R); *Cre* 5′-GAAGCAGAAGCTTAGGAAGATGG-3′ (forward), 5′-TTGGCCCCTTACCATAACTG-3′ (reverse); Internal control 5′- CAAATGTTGCTTGTCTGGTG-3′ (forward); 5′- GTCAGTCGAGTGCACAGTTT-3′ (reverse).

The mice were free to eat and drink under the feeding conditions, such as the temperature of 22 ± 2 °C, humidity: 40 ~ 70%; light cycle: 12 / 12 hours. A total of ten *SND1* LKO male mice were randomly divided into two groups, including the chow diet group (10% kcal from fat, D12450B, Research Diets) (LKO CD) and the high-fat diet group (60% kcal from fat, D12492, Research Diets) (LKO HFD). Meanwhile, the chow diet group (WT CD) and the high-fat diet group (WT HFD) from the ten litters of WT male mice were used as controls. The bodyweight of WT or LKO mice was measured every week.

Mice were killed by dislocation at the 24 w of chow or high-fat diet. Liver tissue and white adipose tissue were quickly separated and weighed. Each liver was divided into three sections: 1) the first fraction was used for the protein extraction for western blot analysis; 2) the second part was weighed and added to the lysate in the kit for the detection of total liver cholesterol (E1015, Applygen, Beijing) and liver free cholesterol (E1016, Applygen, Beijing); 3) the third part was fixed with 10% formalin, then sections of 5–

8 μm were cut out. Liver sections were subjected to Hematoxylin-Eosin (H-E) staining, according to the manufacturer's instructions. An optical microscope was used to capture the images.

Primary hepatocyte extraction

The mice were anesthetized by intraperitoneal injection of 7% chloral hydrate (25 mg/g), approximately 5 min later, the peritoneal cavity was opened. The inferior vena cava was perfused with EGTA solution (E4378, Sigma Aldrich). After the liver became shallow, the portal vein was cut and perfused by the solution of protease (P5147, Sigma Aldrich) and collagenase (C5138, Sigma Aldrich). At the end of the perfusion, a white texture was visible on the liver. After perfusion, the mice were sacrificed and the organ was cut and transferred to a 6 cm culture dish. Pre-warmed protease and collagenase *in vitro* hydrolysate were added, and the tissue was disrupted by forceps. Then, the broken liver tissue was transferred into a 50 ml centrifuge tube and incubated with the 20 ml pre-warmed protease and collagenase in vitro hydrolysate and 1% DNase (D8071, Solarbio) in a 37 °C hybridization chamber for 20 min. The liver tissue was then filtered by the 70 μm pore size Falcon filter (BD Bio-sciences Discovery Labware, Bedford, MA), and centrifuged 20 ~ 30 × g for 4 ~ 5 min at 4 °C. The bottom primary hepatocytes were finally obtained.

Fasting/refeeding assay

After four weeks of chow or high-fat diet in mice, a fasting/refeeding assay was performed. Briefly, mice were fasted for 16 h, and the fasting blood glucose was measured using a blood glucose meter (Accu-Chek Active, Roche). After the chow diet was restored, the blood glucose levels were measured at 0.5 h, 1 h, 2 h, 4 h, and 6 h, respectively. The area under the curve (AUC) was also calculated for the assessment of alteration of blood glucose.

Glucose and insulin tolerance test

At the 4 w, 8 w and 12 w of chow or high-fat diet in mice, a glucose tolerance test (GTT) was performed previously described [14]. Briefly, after the fasting treatment for 16 h, the mice were injected intraperitoneally by a glucose solution (1.5 g/kg). The blood glucose levels were then measured at 0 min, 15 min, 30 min, 60 min, 90 min, and 120 min, respectively. In addition, we also performed the insulin tolerance test (ITT) [14] at the 16 w of chow or high-fat diet in mice. Briefly, 0.75 U/kg insulin (I8040, solarbio) was injected intraperitoneally in mice. Then, the blood glucose levels at 0 min, 15 min, 30 min, 45 min, 60 min, and 90 min were measured. The area under the curve (AUC) was also calculated for the assessment of alteration of blood glucose.

Acute insulin response assay

An acute insulin response assay was performed as previously described [14]. Briefly, at 24 w of chow or high-fat diet in mice, SND1 WT and LKO mice were fasted overnight, and anesthetized by intraperitoneal injection of 7% chloral hydrate (25 mg/g). Approximately 5 min later, the abdominal cavity was opened, and the insulin solution (solarbio) was injected into the portal vein. At the point of 0 min and 5 min, a portion of the liver leaves were cut out to extract tissue proteins. And then, the mice were sacrificed The

phosphorylation level of Akt protein under insulin stimulation was detected by western blotting assay, using anti-Akt (1:1000, 9272S, Cell Signaling Technology) and anti-p-Akt (1:1000, 13038S, Cell Signaling Technology) antibodies. Image J 2X software (NIMH, Bethesda, MD, USA) was used for digitizing the band density.

Western blot analysis

A western blotting assay was performed as previously described [6]. Tissue samples, including liver, spleen, pancreas, and kidney, were homogenized in RIPA buffer (R0020, Beyotime) through a fast cell disrupter (Bullet Blender, Next advance). Primary hepatocytes were isolated from male *SND1* WT and LKO mice. HCC cell line SMMC-7721 was provided by Dr. Zhi Yao (Tianjin Medical University). The following antibodies were used: anti-GAPDH (1:5000, 60004-1-Ig, Proteintech Group), anti-β-actin (1:5000, A5441, Sigma-Aldrich). Mouse monoclonal anti-SND1 antibody was used as described previously [8, 11].

ALF mice model

The mice model of ALF was established by the intraperitoneal injection of LPS (5 mg/kg body weight; L2880, Sigma-Aldrich) and D-GalN (100 mg/kg body weight; G0500 Sigma-Aldrich) for 6 h into six SND1 LKO or WT mice. Normal saline (NS) was administered as the control. Serum aminotransferase activities in the blood sample of six mice were measured using an AST detection kit (C010-2, Jiancheng, Nanjing), an ALT detection kit (C009-2, Jiancheng, Nanjing) and a microplate reader (Varioskan Flash, Thermo). Hematoxylin-Eosin (H-E) staining assay was also performed in different groups using Hematoxylin (ZLI-9610, ZSGB-BIO) and eosin (ZLI-9613,ZSGB-BIO), according to the manufacturer' s instructions.

RNA isolation and quantitative RT-PCR

Total RNA was isolated from mouse liver tissues using TRIZOL reagent (15596-026, Invitrogen), and cDNA was synthesized using a Revert Aid First Strand cDNA Synthesis Kit (K1622, Thermo Fisher Scientific). PCRs were performed using the Fast Start Universal SYBR Green Master Mix (Roche Diagnostics) on a StepOne Real-Time PCR System (Applied Biosystems), as described previously [7]. Primers were synthesized by the GENEWIZ Company (China). The primer sequences used were: *IL-1β* 5'-TGGACCTTCCAGGATGAGGACA-3' (forward); 5'-GTTCATCTCGGAGCCTGTAGTG-3' (reverse); *IL-6* 5'-TACCACTTCACAAGTCGGAGGC-3' (forward); 5'-CTGCAAGTGCATCATCGTTGTTC-3' (reverse); *TNF-α* 5'-GGTGCCTATGTCTCAGCCTCTT-3' (forward); 5'-GCCATAGAACTGATGAGAGGGAG-3' (reverse).

Statistical Analysis

Statistical analysis was performed using IBM SPSS Statistics 19 software. Measurement data are expressed as mean ± standard deviation (SD) and compared by independent Student's t-test or one-way analysis of variance (ANOVA), followed by multiple mean comparisons of Least Significant Difference (LSD). A P value < 0.05 was considered a statistically significant difference.

Results

Conditional knockout of SND1 in hepatocytes

To investigate the effects of hepatocyte-specific deletion of *SND1* on liver insulin resistance and acute liver failure, we first constructed *SND1* liver conditional knockout (LKO) mice. As shown in Fig. 1a, we first built the *SND1 Flox/ Flox* mice with the *loxP* allele flanked at the exon 3 of *SND1* gene and purchased the *wt/ wt*-albumin-Cre$^+$ mice, which includes the *wild type* allele and the specific gene sequence for the expression of albumin-induced Cre enzyme. By crossing the two mice, we obtained the *SND1 Flox/ wt*-albumin-Cre$^+$ heterozygous mice with a probability of 1/2. Then, we performed a second round of mating, using the two *SND1 Flox/ wt*-albumin-Cre$^+$ heterozygous mice, to generate the *SND1 Flox/ Flox*-albumin-Cre$^+$ homozygous mice (*SND1* LKO mice) with a probability of 3/16. *SND1 Flox/ Flox* littermates were used as wild type controls.

To verify the successful construction of *SND1* LKO mice, DNA extracted from mouse primary hepatocytes was used for detecting the existence of *SND1 LoxP* sites. As shown in Fig. 1b, we performed the genotyping assay using the mixture of three primers (F1 within intron 2 of *SND1*, F2 within exon 3, and R within intron 3). For the wild-type control mice without LoxP site, *SND1* WT band of 376 bp was detected by the PCR assay using the F2 plus R primers (Fig. 1b, lane 1). Because the *SND1 Flox/Flox* mice contain the LoxP site, the *SND1 Flox* band of 504 bp was produced by the F2 + R primers (Fig. 1b, lane 2). The existence of albumin-Cre in the *SND1 Flox/ Flox*-albumin-Cre$^+$ homozygous mice (#1 and #2) led to the resection of the sequence between the two LoxP sites and the observation of SND1 LKO band of 279 bp through F1 + R primers (Fig. 1b, lane 3 and 4).Internal control gene was detected in all the above mice (Fig. 1b-c).

Next, we extracted the tissues of liver, spleen, pancreas, and kidney from the *SND1* wild type (WT) (#1, #2, #3) and LKO (#4, #5, #6) mice, respectively (Fig. 1d). SMMC-7721 cell lines of *SND1* WT and knockout (KO) were used as the sample controls. The lysates were subjected to SDS-PAGE and then immuno-blotted using anti-SND1 antibody, or anti-β-actin antibody. The data in Fig. 1c showed that SND1 protein was completely deleted in the SMMC-7721 cell lines of *SND1* KO, but not *SND1* WT. However, we only detected the decreased expression of SND1 in the liver tissue of *SND1* LKO (#4, #5, #6) mice, when compared with the *SND1* WT (#1, #2, #3) mice. There is no difference of SND1 expression between *SND1* WT and *SND1* LKO *mice* in the spleen, pancreas, and kidney tissues (Fig. 1d). Considering the albumin protein was specifically expressed in hepatocytes, we further extracted primary hepatocytes from the liver tissue of the mice, and found that SND1 protein was knocked out in the primary hepatocytes of *SND1* LKO mice (Fig. 1e). Figure 1f showed the gross morphology of *SND1* WT and *SND1* LKO mice. These suggested that the mice with the hepatocyte-specific deletion of *SND1* were successfully constructed.

Gross morphology and weight analysis in the absence of hepatic SND1

A total of five *SND1* WT and five *SND1* LKO mice were randomly selected and fed with chow diet (CD). We monitored the bodyweights of WT or LKO mice weekly and did not find a significant difference (Fig. 2a). After 24 w of CD, we measured the weight of liver tissue, and calculate the ratio value of liver weight/

body weight. There is no statistical difference between the *SND1* WT and *SND1* LKO mice (Fig. 2b). We further measured the weight of white adipose tissue (WAT), and calculate the ratio value of WAT weight/ body weight. Similar negative results were obtained in Fig. 2c.

Next, we further investigated the effect of *SND1* liver conditional knockout on the weight of mice with a high fat diet (HFD). We did not observe the significant difference of body weight and liver weight between *SND1* WT HFD and *SND1* LKO HFD mice (Fig. 3a-d). Nevertheless, the absence of hepatic *SND1* can lead to a decreased WAT weight (Fig. 3e, * $P < 0.05$) or the ratio value of WAT weight/body weight (Fig. 3f, ** $P < 0.01$). These suggested that *SND1* liver conditional knockout can affect the weight of white adipose tissue in mice under the condition of a high-fat diet, but not the gross morphology, body weight, and liver weight of mice.

The glucose homeostasis analysis in the absence of hepatic SND1

We analyzed the glucose homeostasis of *SND*1 WT and *SND1* KO mice with a chow diet. A fasting/refeeding assay was performed. After the fasting treatment of mice with 4w CD for 16 h, we restored the chow diet and measured the blood glucose levels at 0 h, 0.5 h, 1 h, 2 h, 4 h, and 6 h, respectively. As shown in Fig. 4a, we did not observe the statistical difference in blood glucose change between *SND1* WT CD and LKO CD mice.

Next, we performed a glucose tolerance test (GTT). After the fasting treatment for 16 h, we injected intraperitoneally 1.5 g/kg glucose solution in the *SDN1* WT or LKO mice with 4 w chow diet, and measured the blood glucose levels at 0 min, 15 min, 30 min, 60 min, 90 min, and 120 min, respectively. We observed similar negative results (Fig. 4b). We further performed the insulin tolerance test (ITT) at the 16 w of chow in mice. The 0.75 U/kg insulin was injected intraperitoneally in the mice, and the blood glucose levels at 0 min, 15 min, 30 min, 45 min, 60 min, and 90 min were measured. As shown in Fig. 4c, compared with the *SND1* WT CD, no increased AUC value was observed in the *SND1* LKO CD. In addition, we performed an acute insulin response assay. At 24 w of CD in mice, *SND1* WT and LKO mice were fasted overnight, and anesthetized. After the injection of the insulin solution, the phosphorylation level of Akt protein in the liver tissue was analyzed by western blotting assay. The data of Fig. 4d indicated an increased phosphorylation level of Akt at the time point of 5 min, compared with 0 min, in the *SND1* WT mice (#1, #2) and *SND1* LKO mice (#3, #4). Nevertheless, no statistical difference of p-Akt/ total Akt ratio was detected between *SND1* WT and *SND1* LKO mice at the time point of 0 min or 5 min (Fig. 4d).

We also performed the fasting/refeeding assay (Fig. 5a), glucose tolerance test (Fig. 5b-d), insulin tolerance test (Fig. 5e) and acute insulin response assay (Fig. 5f) in the *SND1* WT and *SND1* LKO mice with a high-fat diet, respectively. In the acute insulin response assay, the treatment of the insulin solution did not increase the phosphorylation level of Akt protein (Fig. 5f), suggesting that high-fat diet results in the occurrence of insulin resistance in *SND1* WT and *SND1* LKO mice. We did not observe the positive results (Fig. 5). Taken together, *SND1* liver conditional knockout fails to influence the glucose homeostasis of mice under the condition of a chow diet or high-fat diet.

Cholesterol level and hepatic steatosis analysis in the absence of hepatic SND1

Very recently, we found that SND1 can regulate cholesterol metabolism in mice through promoting the activity of sterol-regulatory element-binding protein 2 (SREBP2) protein during the induction of a high fat diet [14]. In hepatocellular carcinoma (HCC), the up-regulation of SND1 expression also can influence the cellular cholesterol distribution and homeostasis [23]. Thus, we attempted to measure the level of cholesterol in *SND1* WT and LKO mice. As shown in Fig. 6a-c, an increased level of serum total cholesterol, liver free cholesterol, but not liver total cholesterol, was detected in the HFD mice, compared with CD mice. However, we did not observe the statistical difference of the cholesterol level between *SND1* WT and *SND1* LKO mice with chow or high-fat diets. Moreover, the Hematoxylin-Eosin (H-E) staining of liver sections (Fig. 6d) indicated a significant increase in fat vacuoles in the HFD mice, compared with CD mice, but not a remarkable difference between *SND1* WT and *SND1* LKO mice. These suggested that hepatocyte-specific deletion of *SND1* failed to influence the cholesterol level and hepatic steatosis of mice.

Hepatic failure analysis in the absence of hepatic SND1

First, we analyzed the effect of SND1 hepatocyte-specific deletion in the serum levels of ALT or AST. As shown in Fig. 7a, there is an increased level of ALT in both WT and LKO mice (* $P < 0.05$) after 6 h of LPS/D-GalN stimulation, compared with the normal saline (NS) control group. Nevertheless, we did not detect the significant difference between WT and LKO mice (Fig. 7a). We also observed that LPS/D-GalN stimulation led to an increase AST level in the WT mice (* $P < 0.05$), but not LKO mice (Fig. 7b). Furthermore, we performed the quantitative RT-PCR assay to detect the expression level of inflammatory cytokines, including IL-6, IL-1β, and TNF-α. As shown in Fig. 7c, the LPS/D-GalN treatment can induce an enhanced level of *IL-6* expression in both WT (** $P < 0.01$) and LKO (* $P < 0.05$) mice. However, no difference exists in the presence and absence of hepatic *SND1* (Fig. 7c). The similar results were observed for the detection of *IL-1β* (Fig. 7d, *** $P < 0.001$ for WT, ** $P < 0.01$ for LKO) and *TNF-α* (Fig. 7e, ** $P < 0.01$ for WT; * $P < 0.05$ for LKO).

In addition, we performed a Hematoxylin-Eosin (H-E) staining assay to detect the influence of LPS/D-GalN in the histomorphology of liver tissue and investigated whether the deletion of SND1 can affect the role of LPS/D-GalN in the liver tissue damage. As shown in Fig. 7f, LPS/D-GalN treatment results in a significant liver damages (e.g., liver tissue hemorrhage, inflammatory cell infiltration) in LKO mice, compared with the WT mice. Nevertheless, we did not observe the remarkable difference regarding the liver damage extent between WT and LKO mice. These suggested that hepatocyte-specific deletion of *SND1* failed to influence the hepatic failure process of mice remarkably.

Discussion

Insulin inhibits the lipolysis, reduce the delivery of glycerol to the liver, and the conversion of glycerol to glucose [24–26]. Abnormal lipid metabolism is associated with the occurrence of insulin resistance [27, 28]. The accumulation of ectopic lipid in the liver and skeletal muscle can trigger a pathway of inhibiting

the signal transduction of insulin, and result in the reduced muscle glucose uptake and hepatic glycogen synthesis [29]. Previously, we utilized the high-fat diet to establish the mice model of insulin resistance and observed an improved fatty liver and insulin resistance induced by a high-fat diet in the global SND1 transgenic mice [14]. Hepatocytes are responsible for lipogenesis, cholesterol biosynthesis, and glucose metabolism [30]. Here, we aimed at further investigating whether the hepatocyte-specific deletion of SND1 in mice affects the presence of insulin resistance induced by a high-fat diet.

Hepatocyte-specific gene knockout mice are useful to analyze the potential role of the target gene in liver-related diseases. For instance, the complete depletion of tumor necrosis factor receptor-associated ubiquitous scaffolding and signaling protein (TRUSS) in hepatocytes can improve the hepatic steatosis, insulin resistance, glucose intolerance, and inflammatory responses of mice [31]. In this study, we successfully constructed SND1 liver-specific knockout mice for the first time and established high fat diet-induced insulin resistance and LPS/GalN-induced acute liver failure model. Nevertheless, we did not observe the significant difference in insulin resistance and hepatic failure between SND1 WT and SND1 LKO mice. Notably, in our previous study, compared to WT mice, HFD-transgenic exhibited reductions in hepatic steatosis and systemic insulin resistance. HFD-WT mice displayed islet hypertrophy and suppression of glucose induced insulin secretion from islets [14]. This finding suggests that the improved pancreatic metabolism of HFD-transgenic mice is related to the systemic effect of insulin resistance, not to the autonomous influence of pancreatic cells [14]. It is possible that the synergistic action of multiple organs with SND1 contribute to the change of the metabolic phenotype.

The main target organs of insulin action include muscle, liver, and adipose tissue, which take part in the promotion of glucose uptake and the inhibition of glucose production [15]. Ectopic lipids-included insulin resistance in muscle tissue precedes the hepatic insulin resistance and can transfer the ingested glucose to the liver, leading to increased liver fat production and hyperlipidemia [32, 33]. In this study, we observed the decreased weight of white adipose tissue in the *SND1* liver conditional knockout mice under the condition of a high-fat diet, but not the gross morphology, body weight, and liver weight. Although the hepatocyte-specific deletion of *SND1* does not influence remarkably the presence of insulin resistance, it is still meaningful to further analyze the potential effects of *SND1* in adipose or muscle tissues. In addition, we observed the high expression level of *SND1* in the pancreas tissue. More experiments are needed to study the potential role of high-expressed *SND1* pancreas in the glucose homeostasis and hepatic steatosis.

Some studies hint the potential link between cholesterol metabolism and SND1 expression. Based on the global SND1 transgenic mice, we previously identified the promotive role of SND1 in cholesterol homeostasis, only under the treatment of a high-fat diet but not the chow diet [14]. By comparison between the chow- and HFD-fed conditions, we have shown that the improved cholesterol homeostasis in HFD-fed transgenic mice with a higher expression level of the cholesterol metabolic genes in the liver is attributable to the less repressive effect on the cholesterol pathway caused by HFD instead of an inductive influence [14]. The hepatic and global insulin sensitivity derived from HFD-transgenic mice is likely to benefit and dominate cholesterol homeostasis rather than hepatic SND1 itself, which rendered us

to speculate the dispensable role of SND1 from normal hepatocytes in regulating cholesterols. In line with our previous data, this study show no alteration of cholesterols when SND1 is difficient in hepatocytes. Intriguingly, some studies on malignant hepatic cells have shown the opposite. In hepatocellular carcinoma, the up-regulation of SND1 expression can influence the cellular cholesterol distribution and homeostasis [23]. The overexpression of SND1 protein in hepatoma cells contributes to the accumulation of cholesteryl esters, which may result in more cholesterol esterification via fatty acid, and the limitation of triglyceride synthesis [34]. This phenomenon was not observed here in the *SND1* liver-specific knockout mice. How to explain this? We believe metabolic reprogramming is essential for maintaining the growth and proliferation of cancer cell [35], which may partly explain the difference between hepatoma cells and mice normal hepatocyte.

LPS from gram-negative bacteria is implicated in the pathogenesis of ALF [36]. LPS interacts with CD14 and Toll-like receptor 4 (TLR4) to activate inflammatory signals and induce secretion of pro-inflammatory cytokines, which stimulates the infiltration of inflammatory cells into the liver [37–39]. And SND1 was reportedly associated with activation of NF-κB, which results in a chronic inflammatory state leading to HCC [13, 40–42]. Here, we aimed at further investigating whether the hepatocyte-specific deletion of SND1in mice affects the presence of acute liver failure induced by LPS/GalN. Our results did not show the remarkable difference for the LPS/GalN-induced secretion of the pro-inflammatory cytokines (IL-1β, IL-6, and TNF-α) and acute liver failure histomorphology between SND1 WT and LKO mice. Upon stimulation by LPS, the liver resident macrophages, named Kupffer cells (KC) mainly initiate the inflammatory response by secreting pro-inflammatory cytokines, such as IL-1β,IL-6, and TNF-α [43, 44]. The SND1 expression of nonparenchymal cells in SND1 LKO mice may partly explain the negative results. Although hepatocyte-specific deletion of SND1 does not influence remarkably the presence of acute liver failure, it is still meaningful to further analyze the potential effects of SND1 in the global deletion mice upon more acute stimulation.

Conclusion

In summary, our results suggested that hepatocyte-specific deletion of *SND1* failed to affect the high-fat diet-induced insulin resistance or LPS/D-GalN-induced acute liver failure in mice. The synergistic mechanism of multiple organs regarding the role of SND1 in the glucose metabolism, insulin sensitivity, and inflammatory response still merits further experiments.

Abbreviations

SND1, staphylococcal nuclease and tudor domain containing 1; ALF, acute liver failure; LPS, Lipopolysaccharide; GalN, galactosamine; WT, wild type; LKO, liver conditional knockout; CD, chow diet; HFD, high-fat diet; H-E, Hematoxylin-Eosin; NS, Normal saline; LSD, Least Significant Difference.

Declarations

Ethics statement

The study protocols and use of animals were approved by the Institutional Animal Care and Use Committee of Tianjin Medical University.

Consent for publication

Availability of data and materials

The datasets used and/or analyzed during the current study are available from the corresponding author on reasonable request.

Competing interests

The authors don't have conflicts of Interest.

Funding

The reagents, consumables and animal related expenses were supported by grants from the Innovation Team Development Plan of the Ministry of Education (IRT13085 to Jie Yang), National Nature Science Foundation of China (31670759 to Jie Yang, 31571380 to Xingjie Gao), Excellent Talent Project of Tianjin Medical University (to Jie Yang).

Authors' contributions

YJ, WXT and GXJ designed the research; ZCY, CXT, QBX and ZN performed the research; YJ, WXT and GXJ analyzed the data; ZCY, WXT and GXJ wrote the paper; YJ critically revised the manuscript for important intellectual content; XLB and HCB provided administrative, technical, or material support; YJ supervised the study.

Acknowledgements

Not applicable.

References

1. Gutierrez-Beltran E, Denisenko TV, Zhivotovsky B, Bozhkov PV: **Tudor staphylococcal nuclease: biochemistry and functions**. *Cell Death Differ* 2016, **23**:1739-1748.

2. Shaw N, Zhao M, Cheng C, Xu H, Saarikettu J, Li Y, Da Y, Yao Z, Silvennoinen O, Yang J *et al*: **The multifunctional human p100 protein 'hooks' methylated ligands**. *Nat Struct Mol Biol* 2007, **14**:779-784.
3. Duan Z, Zhao X, Fu X, Su C, Xin L, Saarikettu J, Yang X, Yao Z, Silvennoinen O, Wei M *et al*: **Tudor-SN, a novel coactivator of peroxisome proliferator-activated receptor gamma protein, is essential for adipogenesis**. *J Biol Chem* 2014, **289**:8364-8374.
4. Gao X, Fu X, Song J, Zhang Y, Cui X, Su C, Ge L, Shao J, Xin L, Saarikettu J *et al*: **Poly(A)(+) mRNA-binding protein Tudor-SN regulates stress granules aggregation dynamics**. *FEBS J* 2015, **282**:874-890.
5. Gao X, Zhao X, Zhu Y, He J, Shao J, Su C, Zhang Y, Zhang W, Saarikettu J, Silvennoinen O *et al*: **Tudor staphylococcal nuclease (Tudor-SN) participates in small ribonucleoprotein (snRNP) assembly via interacting with symmetrically dimethylated Sm proteins**. *J Biol Chem* 2012, **287**:18130-18141.
6. Su C, Zhang C, Tecle A, Fu X, He J, Song J, Zhang W, Sun X, Ren Y, Silvennoinen O *et al*: **Tudor staphylococcal nuclease (Tudor-SN), a novel regulator facilitating G1/S phase transition, acting as a co-activator of E2F-1 in cell cycle regulation**. *J Biol Chem* 2015, **290**:7208-7220.
7. Yu L, Liu X, Cui K, Di Y, Xin L, Sun X, Zhang W, Yang X, Wei M, Yao Z *et al*: **SND1 Acts Downstream of TGFbeta1 and Upstream of Smurf1 to Promote Breast Cancer Metastasis**. *Cancer Res* 2015, **75**:1275-1286.
8. Su C, Gao X, Yang W, Zhao Y, Fu X, Cui X, Zhang C, Xin L, Ren Y, Li L *et al*: **Phosphorylation of Tudor-SN, a novel substrate of JNK, is involved in the efficient recruitment of Tudor-SN into stress granules**. *Biochim Biophys Acta Mol Cell Res* 2017, **1864**:562-571.
9. Fu X, Zhang C, Meng H, Zhang K, Shi L, Cao C, Wang Y, Su C, Xin L, Ren Y *et al*: **Oncoprotein Tudor-SN is a key determinant providing survival advantage under DNA damaging stress**. *Cell Death Differ* 2018, **25**:1625-1637.
10. Yang J, Valineva T, Hong J, Bu T, Yao Z, Jensen ON, Frilander MJ, Silvennoinen O: **Transcriptional co-activator protein p100 interacts with snRNP proteins and facilitates the assembly of the spliceosome**. *Nucleic Acids Res* 2007, **35**:4485-4494.
11. Gao X, Ge L, Shao J, Su C, Zhao H, Saarikettu J, Yao X, Yao Z, Silvennoinen O, Yang J: **Tudor-SN interacts with and co-localizes with G3BP in stress granules under stress conditions**. *FEBS Lett* 2010, **584**:3525-3532.
12. Cui X, Zhao C, Yao X, Qian B, Su C, Ren Y, Yao Z, Gao X, Yang J: **SND1 acts as an anti-apoptotic factor via regulating the expression of lncRNA UCA1 in hepatocellular carcinoma**. *RNA Biol* 2018, **15**:1364-1375.
13. Jariwala N, Rajasekaran D, Mendoza RG, Shen XN, Siddiq A, Akiel MA, Robertson CL, Subler MA, Windle JJ, Fisher PB *et al*: **Oncogenic Role of SND1 in Development and Progression of Hepatocellular Carcinoma**. *Cancer Res* 2017, **77**:3306-3316.
14. Wang X, Xin L, Duan Z, Zuo Z, Wang Y, Ren Y, Zhang W, Sun X, Liu X, Ge L *et al*: **Global Tudor-SN transgenic mice are protected from obesity-induced hepatic steatosis and insulin resistance**. *FASEB J*

2019, **33**:3731-3745.

15. Haeusler RA, McGraw TE, Accili D: **Biochemical and cellular properties of insulin receptor signalling**. *Nat Rev Mol Cell Biol* 2018, **19**:31-44.
16. Bernal W, Wendon J: **Acute liver failure**. *N Engl J Med* 2013, **369**:2525-2534.
17. Yin J, Ding J, Huang L, Tian X, Shi X, Zhi L, Song J, Zhang Y, Gao X, Yao Z *et al*: **SND1 affects proliferation of hepatocellular carcinoma cell line SMMC-7721 by regulating IGFBP3 expression**. *Anat Rec (Hoboken)* 2013, **296**:1568-1575.
18. Yoo BK, Santhekadur PK, Gredler R, Chen D, Emdad L, Bhutia S, Pannell L, Fisher PB, Sarkar D: **Increased RNA-induced silencing complex (RISC) activity contributes to hepatocellular carcinoma**. *Hepatology* 2011, **53**:1538-1548.
19. Palacios L, Ochoa B, Gomez-Lechon MJ, Castell JV, Fresnedo O: **Overexpression of SND p102, a rat homologue of p100 coactivator, promotes the secretion of lipoprotein phospholipids in primary hepatocytes**. *Biochim Biophys Acta* 2006, **1761**:698-708.
20. Garcia-Arcos I, Rueda Y, Gonzalez-Kother P, Palacios L, Ochoa B, Fresnedo O: **Association of SND1 protein to low density lipid droplets in liver steatosis**. *J Physiol Biochem* 2010, **66**:73-83.
21. Wang T, Wang Z, Yang P, Xia L, Zhou M, Wang S, Du J, Zhang J: **PER1 prevents excessive innate immune response during endotoxin-induced liver injury through regulation of macrophage recruitment in mice**. *Cell Death Dis* 2016, **7**:e2176.
22. Thawley V: **Acute Liver Injury and Failure**. *Vet Clin North Am Small Anim Pract* 2017, **47**:617-630.
23. Navarro-Imaz H, Rueda Y, Fresnedo O: **SND1 overexpression deregulates cholesterol homeostasis in hepatocellular carcinoma**. *Biochim Biophys Acta* 2016, **1861**:988-996.
24. Levine R, Fritz IB: **The relation of insulin to liver metabolism**. *Diabetes* 1956, **5**:209-219; discussion, 219-222.
25. Perry RJ, Zhang XM, Zhang D, Kumashiro N, Camporez JP, Cline GW, Rothman DL, Shulman GI: **Leptin reverses diabetes by suppression of the hypothalamic-pituitary-adrenal axis**. *Nat Med* 2014, **20**:759-763.
26. Samuel VT, Shulman GI: **The pathogenesis of insulin resistance: integrating signaling pathways and substrate flux**. *J Clin Invest* 2016, **126**:12-22.
27. Birkenfeld AL, Shulman GI: **Nonalcoholic fatty liver disease, hepatic insulin resistance, and type 2 diabetes**. *Hepatology* 2014, **59**:713-723.
28. Perry RJ, Samuel VT, Petersen KF, Shulman GI: **The role of hepatic lipids in hepatic insulin resistance and type 2 diabetes**. *Nature* 2014, **510**:84-91.
29. Petersen KF, Laurent D, Rothman DL, Cline GW, Shulman GI: **Mechanism by which glucose and insulin inhibit net hepatic glycogenolysis in humans**. *J Clin Invest* 1998, **101**:1203-1209.
30. Lebeaupin C, Vallee D, Hazari Y, Hetz C, Chevet E, Bailly-Maitre B: **Endoplasmic reticulum stress signalling and the pathogenesis of non-alcoholic fatty liver disease**. *J Hepatol* 2018, **69**:927-947.

31. Yu CJ, Wang QS, Wu MM, Song BL, Liang C, Lou J, Tang LL, Yu XD, Niu N, Yang X *et al*: **TRUSS Exacerbates NAFLD Development by Promoting IkappaBalpha Degradation in Mice**. *Hepatology* 2018, **68**:1769-1785.
32. Petersen KF, Oral EA, Dufour S, Befroy D, Ariyan C, Yu C, Cline GW, DePaoli AM, Taylor SI, Gorden P *et al*: **Leptin reverses insulin resistance and hepatic steatosis in patients with severe lipodystrophy**. *J Clin Invest* 2002, **109**:1345-1350.
33. Petersen KF, Dufour S, Savage DB, Bilz S, Solomon G, Yonemitsu S, Cline GW, Befroy D, Zemany L, Kahn BB *et al*: **The role of skeletal muscle insulin resistance in the pathogenesis of the metabolic syndrome**. *Proc Natl Acad Sci U S A* 2007, **104**:12587-12594.
34. Navarro-Imaz H, Chico Y, Rueda Y, Fresnedo O: **Channeling of newly synthesized fatty acids to cholesterol esterification limits triglyceride synthesis in SND1-overexpressing hepatoma cells**. *Biochim Biophys Acta Mol Cell Biol Lipids* 2018.
35. Santos CR, Schulze A: **Lipid metabolism in cancer**. *FEBS J* 2012, **279**:2610-2623.
36. Jirillo E, Caccavo D, Magrone T, Piccigallo E, Amati L, Lembo A, Kalis C, Gumenscheimer M: **The role of the liver in the response to LPS: experimental and clinical findings**. *J Endotoxin Res* 2002, **8**:319-327.
37. Wu Z, Han M, Chen T, Yan W, Ning Q: **Acute liver failure: mechanisms of immune-mediated liver injury**. *Liver Int* 2010, **30**:782-794.
38. Claria J, Arroyo V, Moreau R: **The Acute-on-Chronic Liver Failure Syndrome, or When the Innate Immune System Goes Astray**. *J Immunol* 2016, **197**:3755-3761.
39. Kitazawa T, Tsujimoto T, Kawaratani H, Fukui H: **Therapeutic approach to regulate innate immune response by Toll-like receptor 4 antagonist E5564 in rats with D-galactosamine-induced acute severe liver injury**. *J Gastroenterol Hepatol* 2009, **24**:1089-1094.
40. Arretxe E, Armengol S, Mula S, Chico Y, Ochoa B, Martinez MJ: **Profiling of promoter occupancy by the SND1 transcriptional coactivator identifies downstream glycerolipid metabolic genes involved in TNFalpha response in human hepatoma cells**. *Nucleic Acids Res* 2015, **43**:10673-10688.
41. Santhekadur PK, Das SK, Gredler R, Chen D, Srivastava J, Robertson C, Baldwin AS, Jr., Fisher PB, Sarkar D: **Multifunction protein staphylococcal nuclease domain containing 1 (SND1) promotes tumor angiogenesis in human hepatocellular carcinoma through novel pathway that involves nuclear factor kappaB and miR-221**. *J Biol Chem* 2012, **287**:13952-13958.
42. Armengol S, Arretxe E, Rodriguez L, Ochoa B, Chico Y, Martinez MJ: **NF-kappaB, Sp1 and NF-Y as transcriptional regulators of human SND1 gene**. *Biochimie* 2013, **95**:735-742.
43. Mencin A, Kluwe J, Schwabe RF: **Toll-like receptors as targets in chronic liver diseases**. *Gut* 2009, **58**:704-720.
44. Heymann F, Tacke F: **Immunology in the liver–from homeostasis to disease**. *Nat Rev Gastroenterol Hepatol* 2016, **13**:88-110.

Figures

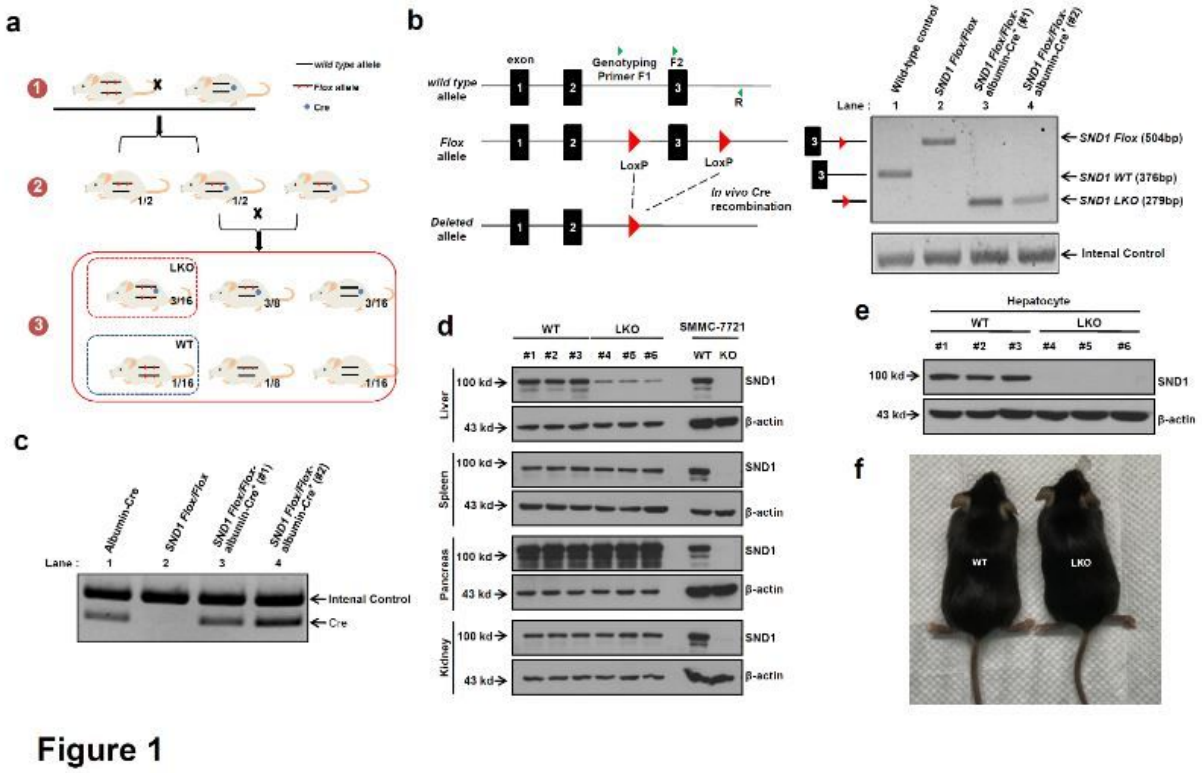

Figure 1

Figure 1

Construction of SND1 liver conditional knockout mice. (a) The mating strategy for the construction of SND1 liver conditional knockout (LKO) mice. The mice were drawn by us. (b-c) We extracted the DNA from mouse primary hepatocytes of the wild-type control, SND1 Flox/Flox, SND1 Flox/Flox-albumin-Cre+ (#1, #2) mice, and performed the genotyping PCR assay. (d) We extracted the tissues of liver, spleen, pancreas, and kidney from the SND1 wild type (WT) (#1, #2, #3) and LKO (#4, #5, #6) mice, respectively. We also used the SMMC-7721 cell lines of SND1 WT and knockout (KO) as the sample controls. The lysates were subjected to SDS-PAGE and then immuno-blotted using anti-SND1 antibody, or anti-β-actin antibody. (e) We also extracted mouse primary hepatocytes for the detection of SND1 expression level, using a western blotting assay. (f) The gross morphology of WT and LKO mice.

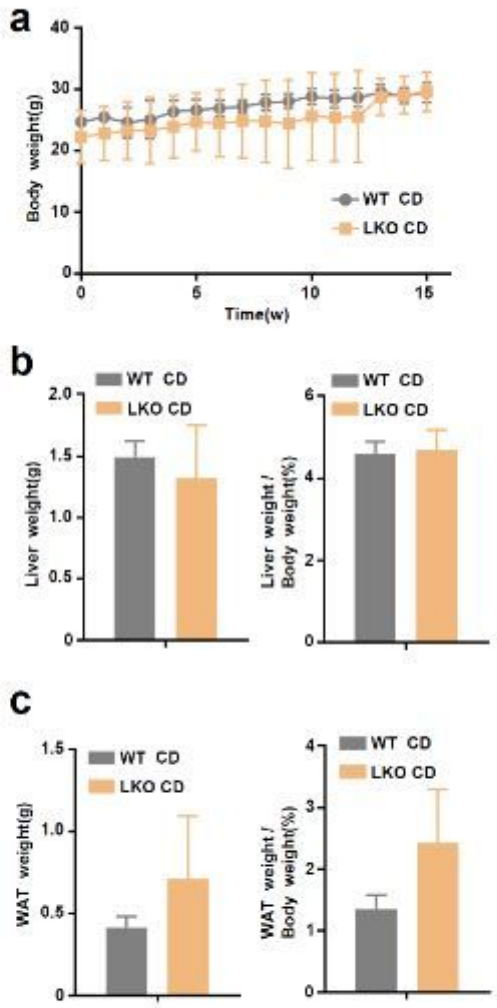

Figure 2

Figure 2

Effect of SND1 hepatocyte-specific deletion on the weight of mice with chow diet. (a) The body weight of WT or LKO mice with chow diet (CD) was measured every week, respectively. (b-c) At the 24 w of CD in mice, the weights of extracted liver tissue and whiteadipose tissue (WAT) were measured, respectively. And the ratio value of liver weight/ body weight, or WAT weight/body weight, was calculated.

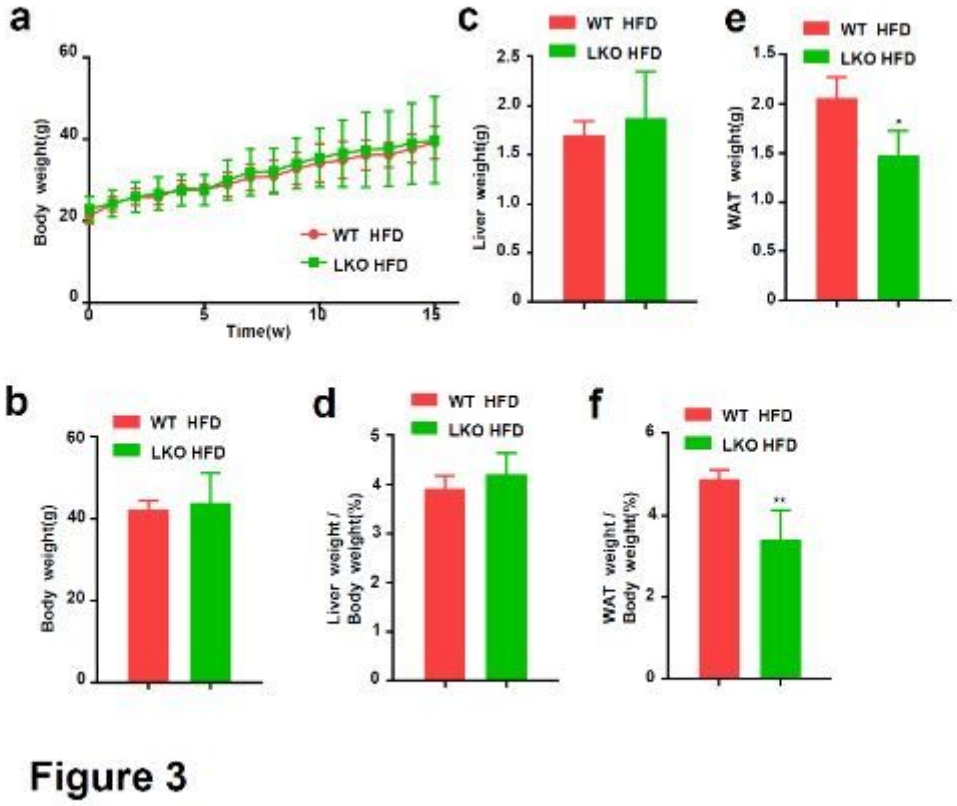

Figure 3

Figure 3

Effect of SND1 hepatocyte-specific deletion on the weight of mice with a high fat diet. (a) The body weight of WT or LKO mice with a high-fat diet (HFD) was measured every week, respectively. (b) At the 24 w of HFD in mice, the body weight was measured. (c-f) The weights of extracted liver tissue and white adipose tissue (WAT) were measured, respectively. And the ratio value of liver weight/ body weight, or WAT weight/body weight, was calculated. An independent-sample Student's t-test was performed, and significant differences were indicated: * $P<0.05$ for the WAT weight of WT HFD vs. LKO HFD; ** $P<0.01$ for the WAT weight/body weight of WT HFD vs. LKO HFD.

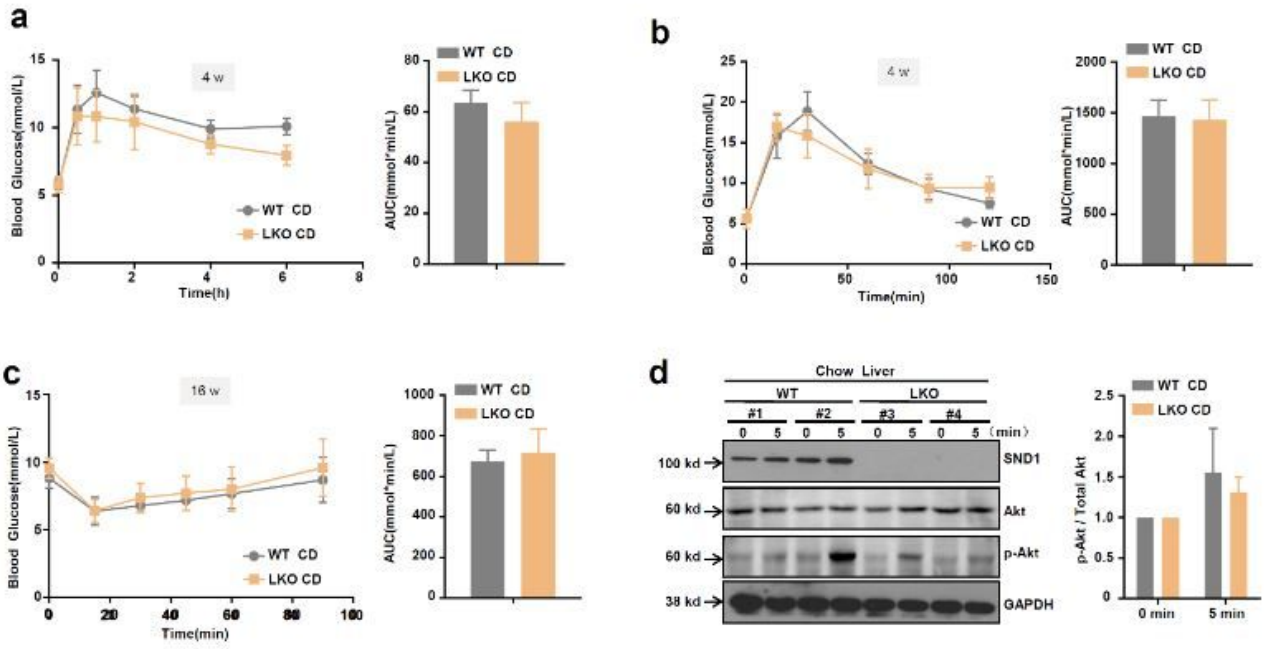

Figure 4

Figure 4

Effect of SND1 hepatocyte-specific deletion on the glucose homeostasis of mice with chow diet. (a) After the fasting treatment of mice with 4w chow diet (CD) for 16 h, the chow diet was restored. The blood glucose levels at 0 h, 0.5 h, 1 h, 2 h, 4 h, and 6 h were measured, respectively. (b) After the fasting treatment for 16 h, 1.5 g/kg glucose solution was injected intraperitoneally in the SDN1 WT or LKO mice with 4 w chow diet. The blood glucose levels at0 min, 15 min, 30 min, 60 min, 90 min, and 120 min were measured, respectively. (c) 0.75 U/kg insulin was injected intraperitoneally in the SDN1 WT or LKO mice with 16 w chow diet. The blood glucose levels at 0 min, 15 min, 30 min, 45 min, 60 min, and 90 min were measured. The area under the curve (AUC) of the above was also calculated, respectively. (d) At the 24 w of chow diet in mice, SND1WT and LKO mice were fasted overnight and anesthetized. After the injection of the insulin solution, the phosphorylation level of Akt protein in the liver tissue was analyzed by western blotting assay at the point of 0 min and 5 min. The band density was digitized by the Image J 2X software.

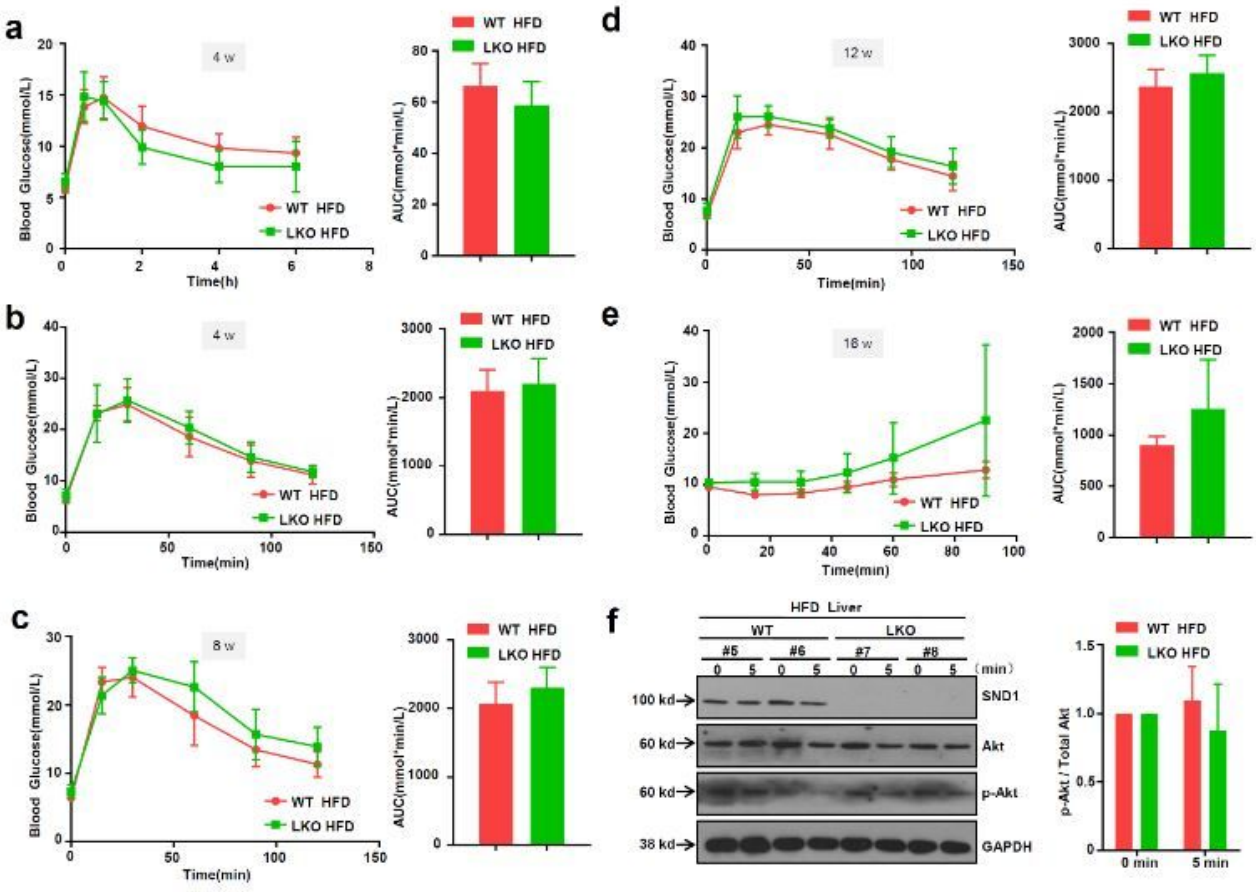

Figure 5

Figure 5

Effect of SND1 hepatocyte-specific deletion on the glucose homeostasis of mice with a high fat diet. (a) After the fasting treatment of WT and LKO mice with 4 w high-fat diet (HFD) for 16 h, the chow diet was restored. The blood glucose levels at 0 h, 0.5 h, 1 h, 2 h, 4 h, and 6 h were measured, respectively. (b-d) After the fasting treatment for 16 h, 1.5 g/kg glucose solution was injected intraperitoneally in the WT, and LKO mice at 4 w, 8 w, 12 w of a high-fat diet. The blood glucose levels at 0 min, 15 min, 30 min, 60 min, 90 min, and 120 min were measured, respectively. (e) 0.75 U/kg insulin was injected intraperitoneally in the WT and LKO mice at 16 w of a high-fat diet. The blood glucose levels at 0 min, 15 min, 30 min, 45 min, 60 min, and 90 min were measured. The area under the curve (AUC) of the above was calculated, respectively. (f) At the 24 w of a high-fat diet in mice, SND1WT and LKO mice were fasted overnight and anesthetized. After the injection of the insulin solution, the phosphorylation level of Akt protein in the liver tissue was analyzed by western blotting assay at the point of 0 min and 5 min. The band density was digitized by the Image J 2X software.

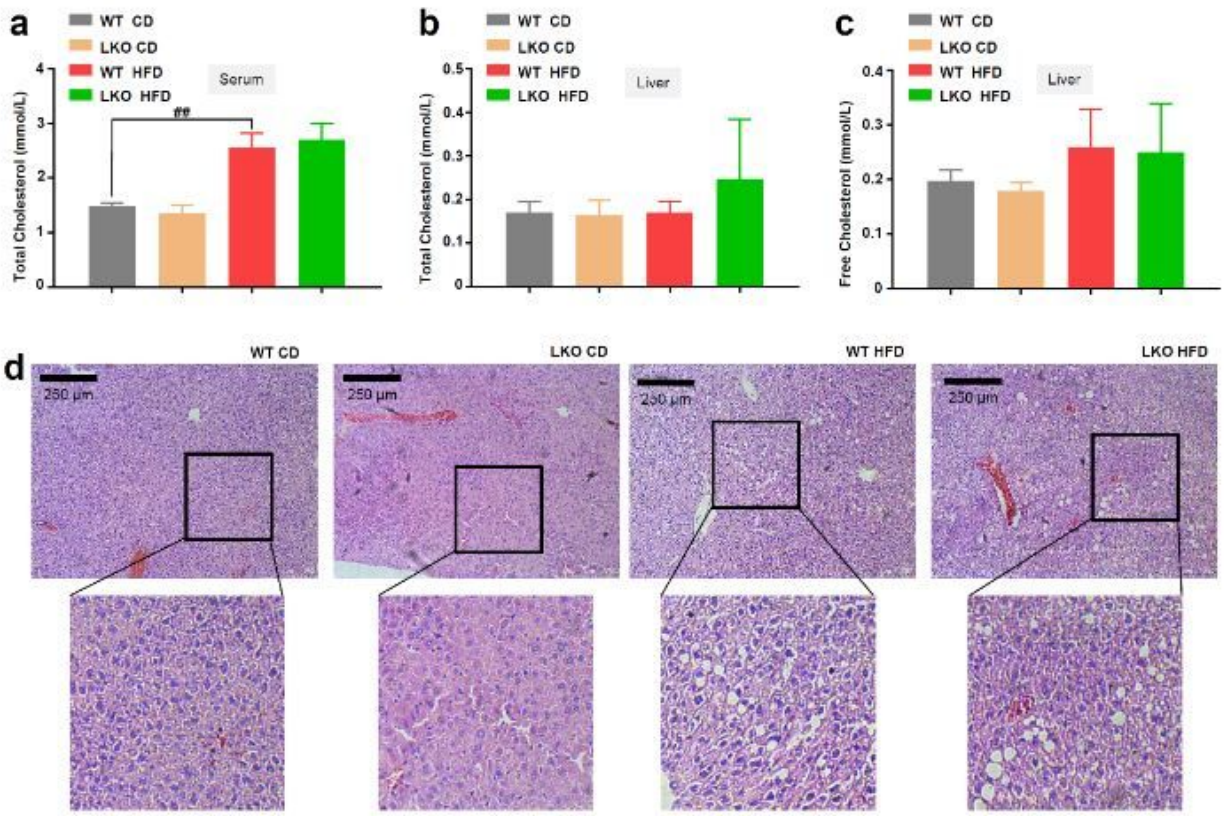

Figure 6

Figure 6

Cholesterol level and hepatic steatosis in WT and LKO mice with a high-fat diet. (a-c) At 24 w of a high-fat diet, the levels of serum total cholesterol, liver total cholesterol, and liver free cholesterol were measured. (d) Liver sections were subjected to Hematoxylin-Eosin (H-E) staining, and images were captured by an optical microscope. Bar, 250μm.

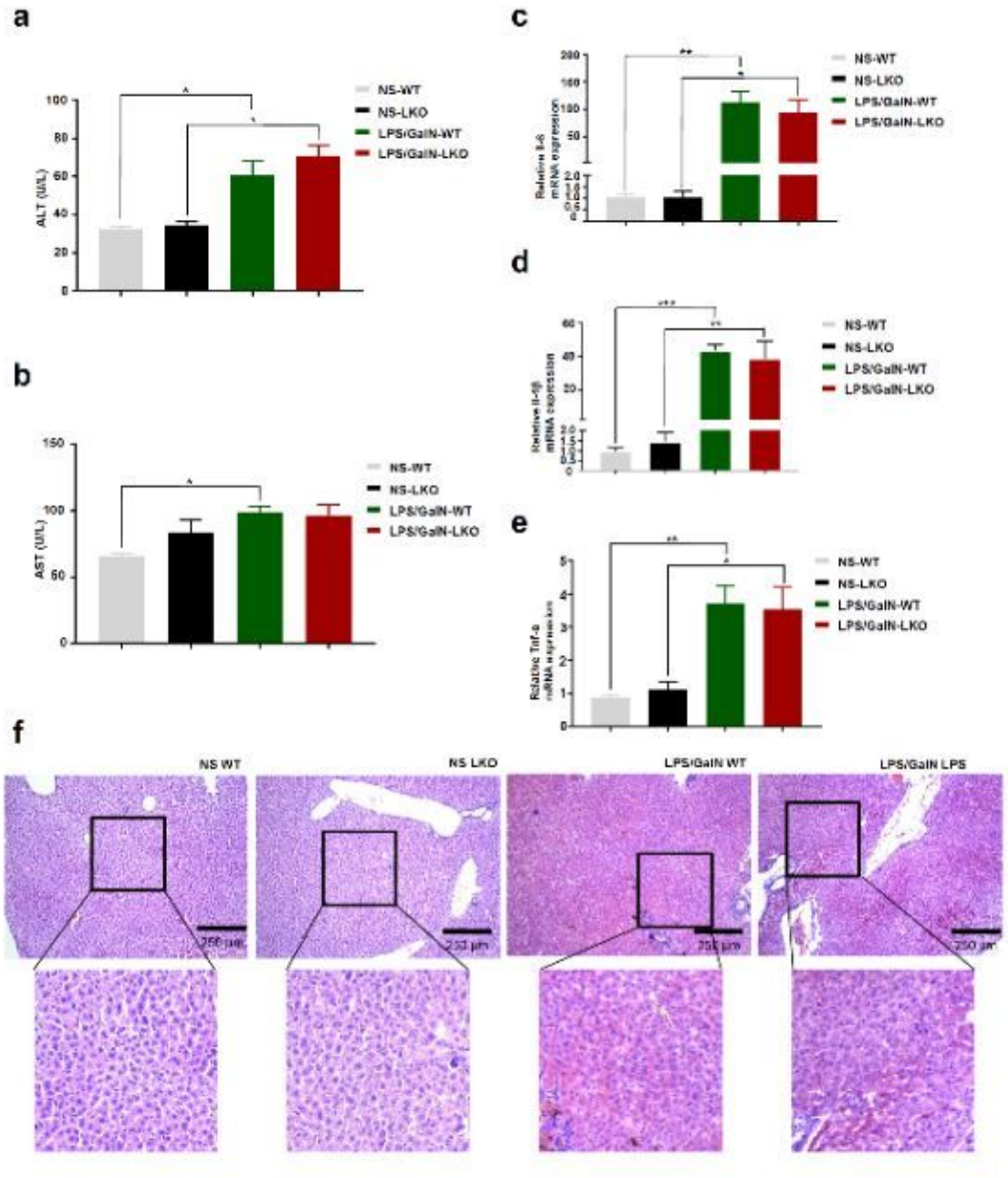

Figure 7

Figure 7

Effect of SND1hepatocyte-specific deletion on the acute liver failure induced by LPS/GalN. WT and LKO mice were administered 5 mg/kg LPS and 100 mg/kg D-GalN intraperitoneally. Normal saline (NS) was administered as the control. Serum activities of ALT (a) and AST (b) were measured at 6 h after LPS/D-GalN treatment. The hepatic mRNA levels of IL-6 (c), IL-1β (d), and TNF-α (e) in the liver tissues were also measured by quantitative RT-PCR. An ANOVA-LSD test was performed, and significant differences were

indicated: * P< 0.05, **P < 0.01, *** P< 0.001. (f) H&E staining images of representative liver samples were presented. Scale bar, 250 μm.

Supplementary Files

This is a list of supplementary files associated with this preprint. Click to download.

- Originalfulllengthgelandblotimages20200713.pdf
- NC3RsARRIVEGuidelinesChecklist201420200703.docx